10TH INTERNATIONAL SYMPOSIUM ON PARTICLE IMAGE VELOCIMETRY – PIV13
Delft, The Netherlands, July 2-4, 2013

Combined 3D Scanning PIV and Scanning LIF for flow and phase transfer measurements around a melting particle

Hess D. [1], Brücker Ch.[1] and Nonn Th.[2]

[1] Institute of Mechanics and Fluid Dynamics, TU Bergakademie Freiberg, Germany
david.hess@tu-freiberg.de, bruecker@imfd.tu-freiberg.de

[2] Dantec Dynamics, Skovlunde, Denmark thomas.nonn@dantecdynamics.com

Abstract Interfacial flow and phase transfer around a melting solid particle were investigated with combined 3D Scanning PIV and Scanning LIF technique. Experiments were carried out with a spherical ice-particle, which was initially shock-frozen from water saturated with fluorescent dye. Flow in a water tank seeded with small tracer particles was investigated, when the ice-particle was released at the water surface in the center of the tank and the melting process began. A scanning light-sheet was generated with a polygonal mirror and flow was recorded with two high-speed cameras with a beam splitter plate. The cameras were equipped with different color filter such that cam#1 recorded only the clean water while cam#2 recorded the molten fluid generated by the heat transfer of the frozen fluorescent ice-particle. This allowed us to record the 3D flow and 3D concentration field simultaneous. The results showed the complexity of induced flow process by the heat/phase transfer and buoyancy interacting with the base flow in the water tank. A small swirl in the tank was enforced by buoyancy-induced vortex stretching and resulted in increasing particle rotation. This self-enforcing process generated a columnar vortex in the wake below the particle which underwent vortex breakdown. Fluid originating from the phase transfer process was accumulated in the vortex.

Introduction

The physics of solid-liquid two-phase flows including physical and chemical transformations is the subject of intense research in many engineering sciences, e.g. in chemistry, metallurgy and geophysics. The basic applications, where solid-liquid flows play the most important role are fluidized beds, sedimentation columns, slurries and mining. Despite of relative good practical experiences, casting technology still remains in an experimental stage due to a lack of fundamental understanding of transport phenomena occurring inside the mushy zone including the transport of fluid, heat and solute in the mixture of molten metal and solid particles. These applications have motivated an increasing number of theoretical and experimental studies of solid-liquid two-phase flows. Due to the micro-scale character of the phase-change process occurring at the interface between the solid and fluid phases, our understanding is mainly based on detailed experiments at the interface and direct numerical simulations (DNS model) for fixed particles in a fluid, the interested reader is referred to the review given by Hoef et al. (2008). However, motion of the particles in the ambient fluid is another aspect which is of importance and requires not only resolving the interfacial flow but the dynamics of the particles and the ambient flow, too.

Hao and Tao (2001) performed an experimental investigation on flow around a non-movable melting ice sphere in horizontally flowing water. The flow field was measured quantitatively using particle image velocimetry (PIV). Additionally for the visualization of convective melting the dyed ice was utilized to study the motion of molten ice and its mixing patterns with the mainstream. Dietrich et al. (2011) made an approach by simulating the melting particles and their interaction. Parallel, the authors performed the comparisons of results with the flow around a non-melting solid sphere in order to study the effect of melting on the boundary layer flow. In particular, it was shown that the ratio between initial Grashof number and Reynolds number Gr/Re is responsible for the shape variation of the ice sphere in the melting process. When Gr/Re is small (less than unity) the shape over the rear ice sphere becomes flat and the overall shape of the ice particle transforms into a scallop. With a high Gr/Re > 6 the shape of the sphere changes into an ellipse.

Later, the same authors investigated the influence of convection on the melting of ice particles moving in a lid driven cavity, see Hao & Tao (2003). Using flow visualization and measurements, the authors determined experimentally the volumes and packing patterns of the melting granular packed beds and the time variation of average melting rate per unit bed volume. In particular, video recordings and digital image processing were used to record the shape deformations. Authors identified two basic types of packing pattern: floating and non-floating packing in dependence on flow conditions. Using the definition of a terminal velocity, a Reynolds number ratio was developed as the criterion that distinguishes the floating, non-floating or transitional packing pattern. In addition, the authors analzed the influence of packing patterns on Nusselt number correlations.

Comprehensive 2D DNS modeling of single cylindrical particles settling and melting in a hot fluid with Prandtl number of Pr = 0.7 has been carried out by Gan et al (2003). It was shown that the melting rate of each particle has a local character and strongly depends on the sedimentation velocity of the particle. However, the influence of particle-particle and particle-wall collisions as well as the hydrodynamic influence of the wall on the particle dynamics was not investigated. Recently Feng et al. (2008) reported about direct numerical simulations of non-isothermal particulate flows for different Grashof numbers. The Prandtl number of the fluid was set to unity. Simulation of two particles demonstrated that heat convection around the particles modifies the drafting-kissing-tumbling (DKT) scenario of their motion. In particular, it was observed that the buoyancy currents induced by the hotter particles reverse the DTK motion of the particles or suppress it altogether. A number of 500 particles rising in an enclosure were recently simulated by Dan & Wachs (2010) including the effect of thermal buoyancy on the fluidization of particles. The computational mesh comprised 10^7 tetrahedral elements, where each particle was resolved using approximately 10-20 nodes on the particle diameter. However, resolution was not sufficient to determine the thermal boundary layer in detail.

To sum up, our understanding of the complex interaction between melting particles and the surrounding fluid and walls is far from being complete. Motivated by this fact, this work presents detailed investigations of the interfacial heat and mass transfer between solid and liquid phase in a reference system of a melting ice-particle in container flow at well-defined boundary conditions. In this work we consider the case of a single melting ice particle placed at the free surface of a water column. Local convection flow is induced due to the temperature gradients caused by the melting of the ice particle and the resulting density difference in the three-dimensional container. The method of combined 3D Scanning PIV and Scanning LIF was used to investigate the flow and phase transfer measurements around the particle.

Experimental Methods

The experiments were carried out in an octagonal water basin with an ice-particle floating on top of the water surface. In order to distinguish the melt flow due to phase-transfer of the ice particle from the flow of the surrounding liquid we marked the particle with fluorescent dye and seeded the water basin with small tracer particles (VESTOSINT®, Hoechst). To generate the ice particle, distilled water used which was mixed homogeneous with rhodamine dye before it was shock-frozen in a spherical mold (diameter 3.5cm). The ice-particle was then carefully launched on the surface of the water column to avoid any flow disturbances. Initially, the water in the basin was at rest. Flow was then generated by the convection in the tank induced by the heat transfer across the particle. It was observed that the particle set into rotational motion after a while which continued until the size of the particle was below a critical value.

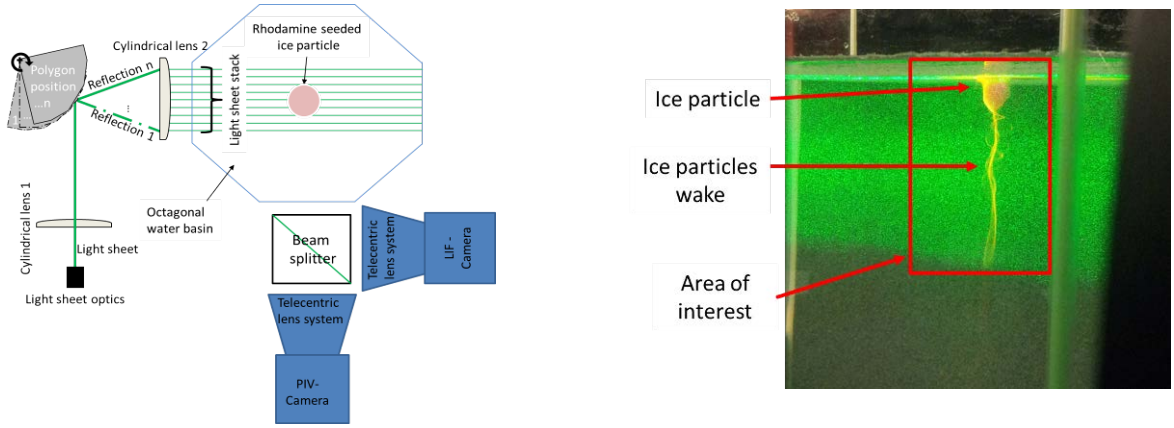

Figure 1: Left: sketch of experimental set-up for combined 3D Scanning PIV and Scanning LIV. Right: picture of the scene with a standard camera from the side during the melting process

In order to capture the 3D fluid motion and the 3D concentration field separately, we used a 2-camera high-speed recording system with different optical filters and the method of light-sheet scanning (figure 1). The illumination was generated by a high speed laser (Litron Nd:YLF laser, 30 mJ at 1 kHz repetition rate, wavelength 527 nm) combined with a polygonal scanner, which rapidly shifted a single light sheet through the volume of interest (Hess et al. 2011). Each light sheet image was captured by the two high speed camera systems simultaneous and along the same optical path, which was realized with a beam splitter plate. The lens systems were equipped with different color filters. One camera obtained images from the tracer particles in the ambient fluid (filter 527 nm ± 10 nm) without any cross-talk

from molten fluid. The other filter blanked out the particles and took only pictures of the concentration of Rhodamine dye (filter 576 nm ± 27 nm) released into the water by the melting process. Note that the diffusion coefficient of the marker is low ($D=3.6 \times 10^{-9}$ m²/s see Rani et al. 2005) such that the diffusive transport is much weaker than convection and phase transfer. An overview of the experimental set-up is shown in figure 1 on the left side. The volume of interest had a size of 102×64×48 mm³ and was scanned by 200 light sheets at frame rate of 6 kHz between each sheet and respectively a volume scan rate of about 25 Hz. The two image sets were stacked together to span a voxel space, see also Hess et al. (2011). The particle volumes were then restructured to obtain isotropic particle representations inside the voxel volumes (Brücker et al. 2013). Two successive particle volumes were then analyzed by using 3D Least-Squares Matching (LSM) to gather information about the 3D flow velocities. A combination of the reconstructed 3D particle field and the 3D rhodamine concentration is given in figure 2. The pictures demonstrate the good quality of particle reconstruction and the structure of the molten fluid in the wake of the ice-particle as visualized with the rhodamine dye.

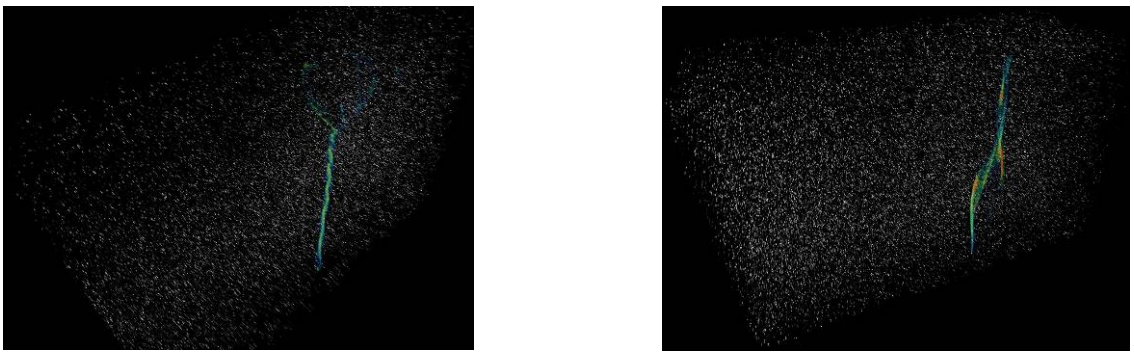

Figure 2: Overlaid image of the reconstructed 3D particle volume and the 3D rhodamine concentration in different levels below the ice-particle. Left: upper edge of volume is below the water surface; right: upper level of the volume is 10cm below the water surface.

Results

A complex interaction of the melting flow with the surrounding liquid is observed. Due to heat transfer and phase change, convection flow is induced downwards along the axis into the wake of the sphere. As a consequence, mass balance requires a radial inflow induced at the upper fluid levels and a circulation flow is induced. Because of small disturbances in the ambient liquid, a small swirl was induced similar to the process generated in a bathtub vortex. The convection flow induces vortex stretching and due to conservation of angular momentum, auto-rotation of the ice-particle is induced and increases over time. This is documented in figure 3. On the other hand, the melting reduces the particle size which finally reduces the induced convection flow. Downstream of the vortex core, one can recognize the so-called phenomenon of vortex breakdown, which is induced by the opposed pressure gradient.

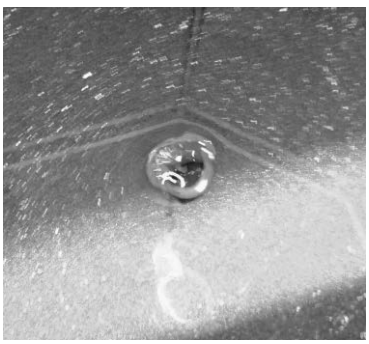

Figure 3: Oblique view on the water surface showing the rotation of the ambient fluid (4 min after release of the ice-particle on the surface). The period of one revolution of the ice-particle is T = 3s.

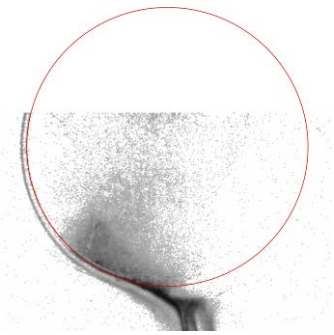

Figure 4: Light-sheet picture of the rhodamine concentration in the center plane of the sphere. A red circle indicates the contour of the sphere and next to it the boundary layer (thickness is about $\delta / D = 0.023$).

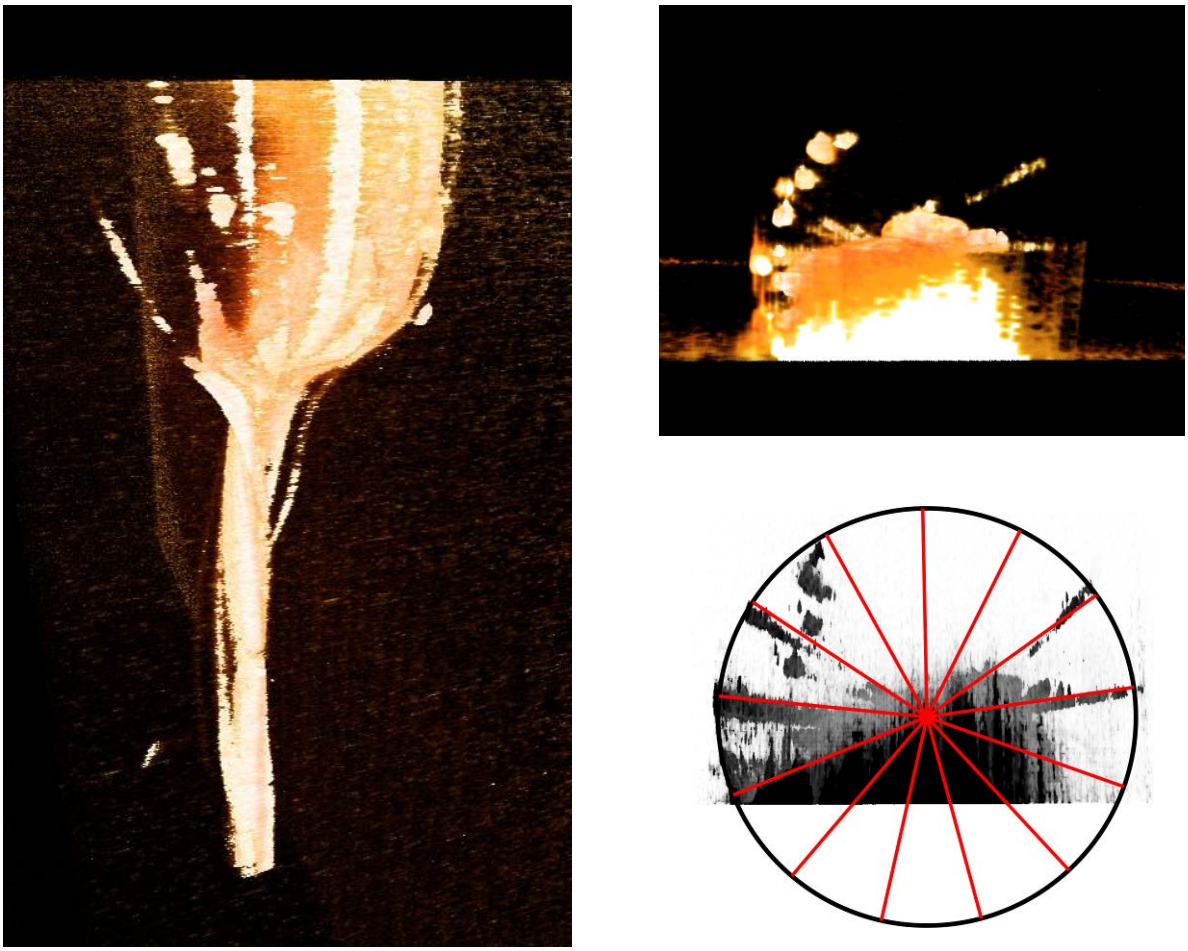

Figure 5: 3D LIF reconstruction of the concentration of molten liquid around the melting ice particle 1 min after release of the particle on the surface of the water column. Left: 3D view, note the ribbon-like areas of rhodamine with high concentrations around the circumference of the sphere. In the top-view (top image on the upper right hand side) one can clearly see an approx. constant angular spacing of those ribbons. The regular behavior is shown in lower image on the right hand side. Between each red line there is an angular displacement of $\Delta\theta \approx 27.7°$.

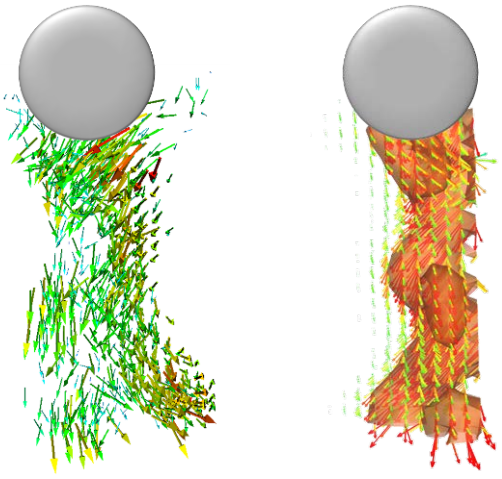

Figure 6: Reconstructed 3D velocity field in the wake of the sphere (only velocity vectors larger than 0.007 m/s are plotted). Left: velocity vector fields, right: surface of constant vertical velocity. Note the double-helical structure of the surface.

Major interest was the development of flow instabilities around the particle and the structure of the resulting convection flow. Figures 5 and 6 show the 3D LIF and 3D PIV results approx. 1 min after the particle was put in the basin and Figs. 7,8 show the results about 3 minutes later. Around the sphere, fluid cools down and moves deeper into the basin together with the molten ice in a vertical column. The typical convection velocity is in the order of 1 cm/s and the resulting Biot number is about 13 (estimated from alpha conditions in a simple convection flow in water). The results in fig. 6 show such a vertical transport below the sphere down into the deeper levels of the basin. Only regions of high velocities in vertical direction (larger than 0.007m/s) are shown and the resulting flow region clearly shows the columnar structure. Interestingly, the 3D LIF reconstruction shows a regular pattern of regions of high concentrations of molten fluid around the sphere along the circumference. These regions look like ribbons arranged along the longitudinal lines of the sphere. A rough estimation of the wavelength of the structures gives a value of $\lambda/\pi D = 1/13$. Note that most of the ribbons seem to originate from the upper part near the contact line of the sphere with the water surface. However, there are also other ribbons which originate in deeper layers of the sphere

below the water surface. Molten fluid is transported along these ribbons down into the wake of the sphere where the ribbons intertwine and form a pigtail-like columnar wake.

This type of sink flow leads to the generation of swirl similar to a bathtub vortex. As a result, the ice-particle starts to rotate around its axis while melting. The rotation is still weak after 1 minute but it increases to about 20 rpm after 4 minutes. Results for the later state are given in Fig. 7 and 8. Herein one can recognize in the vertical cross-section the circulatory flow induced around the sphere with inwards motion in the upper layers and downwards directed motion below the sphere. On the other hand, the flow in the horizontal cross-section clearly reveals are swirling flow. The 3D LIV reconstructions indicated the swirl by means of the strong intertwining of the ribbons. In the vertical cross-section, the structures show the pattern of Christmas tree. The flow field along the axis of the tree let recognize a spiral-type pattern which is wound around the tree. This hints on the presence of spiral type instabilities that deform the axis of the bathtub vortex similar as in spiral-type vortex breakdown. This phenomenon needs further investigation of the flow details which is beyond the paper.

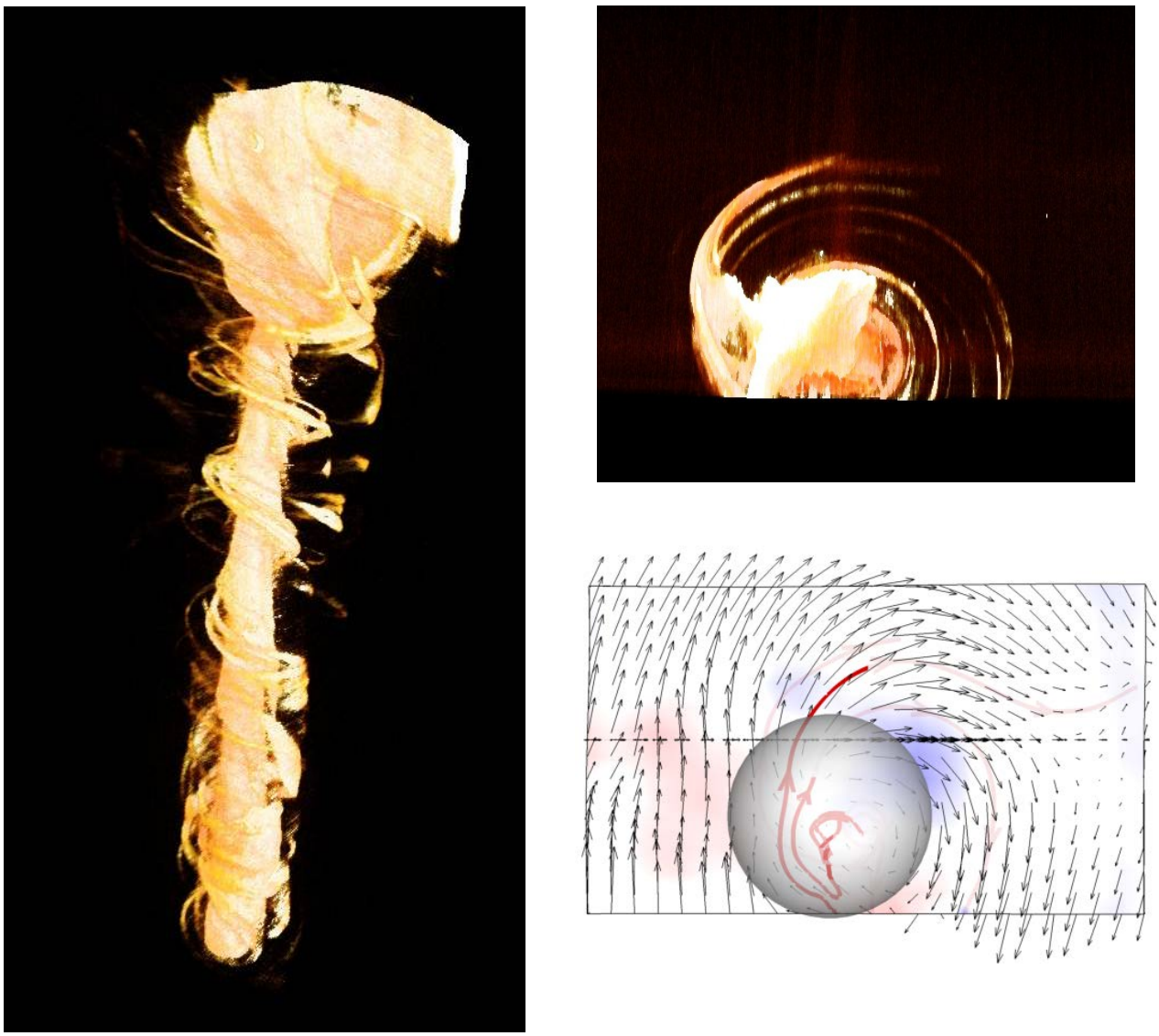

Figure 7: 3D LIF reconstruction of Rhodamine concentration and 3D PIV velocity field in the wake of the ice-particle at 4min after release of the particle on the water surface. Left: 3D view, note the intertwining and folding of the ribbons in the wake. The rotation of the flow leads to separation of the ribbons from the surface of the sphere where they wind around the center part of the sink flow. In the topview (top image on the right hand side) one can see the circular arrangements of different ribbons around the circumference. The flow in the horizontal cross-section below the sphere shows the swirl motion induced by the sink flow.

A closer look into the structure of the wake is given Figure 8. It is seen that sheets of concentrated molten fluid separate from the sphere surface near to the equator and are transported down into the wake. The induced convection flow brings

those sheets closer to the axis and vortex stretching finally concentrates the fluid along the axis. Therefore the LIF structures show a pattern typical for the cut through an earpiece. On the other hand, the flow fields show that the convection flow in the wake is not axisymmetric but reveals a spiral-type pattern

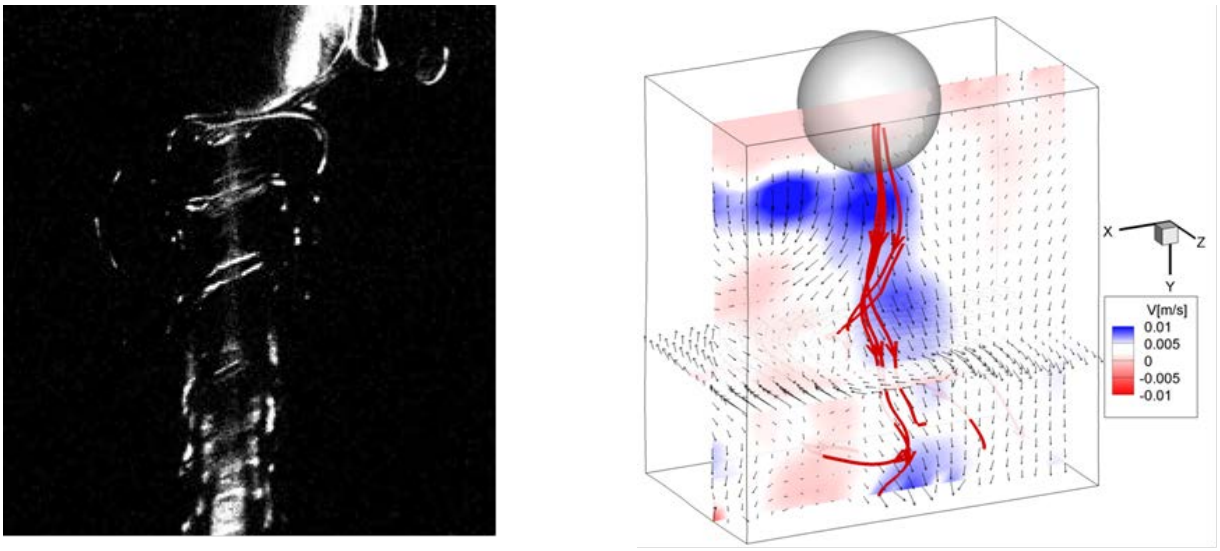

Figure 8: 3D Flow structure in the wake of the ice-particle. Left: cut through the center of the wake out of the 3D LIF reconstruction; right: structure of the sink flow shown by 3D streamlines, vector fields and regions of low and high vertical velocity (blue: downwards flow, red: weak upwards flow in vertical direction).

Discussion and conclusion

The present work describes the analysis of the 3D flow and concentration field for the convection flow induced by a melting ice-sphere on the surface of a water basin. The method of combined 3D Scanning LIF and 3D Scanning PIV is applied to determine both, the flow and concentration field of the molten part of the ice-sphere. This method allowed us to reconstruct a final-scale instability induced near the surface of the sphere and its relation to the induced convection flow. The Prandtl number of the flow is about 7 and the Biot number is 7. Initial temperature difference is 20°C.

A major result is the observation of induced auto-rotation of the particle as a consequence of the generation of swirling motion similar to a bathtub-like vortex. This is driven by the sink flow below the particle where cold fluid is transported in deeper layers of the basin and mass conservation requires that inwards directed flow is generated at the upper layer near the surface. Small disturbances in the ambient fluid are brought to the axis where conservation of angular momentum and vortex stretching lead to formation of a swirling motion in the tank after a certain period of time. The resulting flow field below the sphere let recognize spiral-type motion patterns around the axis which hints on a possible relevance of helical instabilities that are connected with the phenomenon of spiral-type vortex breakdown.

Furthermore, the results show that the molten fluid in the boundary layer of the sphere accumulates in ribbon-like structures with a regular pattern around the circumference of the sphere. This instability is assumed to be a consequence of the interplay of Marangoni-convection at the surface and 3D Taylor-Couette vortices generated around the circumference of the rotating sphere. The initial location of the ribbons is dominated by the Marangoni-convection. The weak rotation of the sphere induces a radial pressure gradient which acts on the particles around the sphere. Because of the density differences between the liquid layers of ambient fluid and molten fluid the latter heavier fluid is forced to move radially outwards against the radial pressure gradient. This centrifugal instability known as Taylor-Couette instability in rotating system may generate small vortex pairs along the longitudinal line of the sphere where the molten fluid is accumulated and transported downwards into the wake. The present results give a first impression of the complexity of this behavior. A detailed analysis of the process under variations of the boundary conditions is necessary to further elucidate the physics of this process in detail which is part of ongoing work.

Acknowledgements

The authors appreciate the financial support of the Government of Saxony and the Federal Ministry of Education and Science of the Federal Republic of Germany as a part of the Centre of Innovation Competence VIRTUHCON.

References

Brücker Ch, Hess D, Kitzhofer J (2013) "Single-View Volumetric PIV via High-Resolution Scanning, isotropic voxel restructuring and 3D Least-Squares Matching (3D-LSM)" , Meas Sci Technol 24 024001 (2013) doi:10.1088/0957-0233/24/2/024001

Brücker Ch (1999) "Structure and dynamics of the wake of bubbles and its relevance for bubble interaction", Phys Fluids 11, 1781-1796.

Brücker Ch (2000) "PIV in multiphase flows", In: Particle Image Velocimetry and Associated Techniques. VKI Lecture Series, 2000-01.

Dan C & Wachs A (2010) "Direct Numerical Simulation of particulate flow with heat transfer", Int J Heat Fluid Flow 31, 1050–1057.

Dierich F, Nikrityuk P.A, Ananiev S(2011) "2D modeling of moving particles with phase-change effect" Chemical Engineering Science. p. 5459-5473

Feng ZG & and Michaelides EE (2009) "Heat transfer in particulate flows with direct numerical simulation". Int. J. Heat Mass Transfer, 52:777–786, 2009.

Gan H, Feng JJ, & Hu HH (2003) "Simulation of the sedimentation of melting solid particles". Int J Multiphase Flow 29(5), 751–769.

Hao YL & Tao YX (2001) "Melting of a solid sphere under forced and mixed convection: flow characteristics". J. Heat Transfer 123, 930–950.

Hao YL & Tao YX (2003) "Non-thermal equilibrium melting of granular packed bedin horizontal forced convection. Part I: experiment" International Journal of Heat and Mass Transfer 46, 5017–5030.

Hess D, Brücker Ch, Kitzhofer J, Nonn T (2011) "Single-View Volumetric PIV using High-resolution Scanning and Least Squares Matching". 9th Int. Symp. Particle Image Velocimetry – PIV'11. Kobe, Japan, July 21-23, 2011

Hoef, van der MA, Annaland, van Sint M, Deen NG, & Kuipers JAM (2008) "Numerical Simulation of Dense Gas-Solid Fluidized Beds: A Multiscale Modeling Strategy", Ann Rev Fluid Mech 40, 47-70.

Rani SA, Pitts B, Stewart PS (2005) " Rapid Diffusion of Fluorescent Tracers into Staphylococcus epidermidis Biofilms Visualized by Time Lapse Microscopy". Antimicrob Agents Chemother 49(2), 728-732.